

# The Atmospheric Pollution Influence on the Surface Structures of Porous Geomaterials in Correlation with Some Natural Radionuclides

VASILE PELIN<sup>1</sup>, IULIANA GABRIELA BREABAN<sup>2,3\*</sup>, ION SANDU<sup>4,5\*</sup>, SILVIU GURLUF<sup>3,6</sup>

<sup>1</sup> Alexandru Ioan Cuza University, Faculty of Geography and Geology, Environment Science Department, Doctoral School of Chemistry, Life Sciences and Earth, 20A Carol I Blvd., 700506, Iasi, Romania

<sup>2</sup> Alexandru Ioan Cuza University, Faculty of Geography and Geology, Geography Department, 20A Carol I Blvd., 700506, Iasi, Romania

<sup>3</sup> Alexandru Ioan Cuza University, CERNESIM Department, 11 Carol I Blvd., 700506, Iasi, Romania

<sup>4</sup> Alexandru Ioan Cuza University, ARHEOINVEST Interdisciplinary Platform, 11 Carol I Blvd., 700506, Iasi, Romania

<sup>5</sup> Romanian Inventors Forum, 3 Sf. Petru Movila Str., 700089 Iasi, Romania

<sup>6</sup> Alexandru Ioan Cuza University, Faculty of Physics, Atmosphere Optics, Spectroscopy and Lasers Laboratory - LOASL, 11 Carol I Blvd., 700506, Iasi, Romania

*In the current context of climate and environmental changes, knowledge on the degradation and deterioration of the geomaterials mechanisms existing in the structure of both buildings and historical monuments becomes a priority due to the influence of atmospheric pollutants on apparent lithic surfaces. The aim of the paper is to highlight the impact of pollution on the surface structures of some porous carbonate rocks, where a series of radionuclides and heavy metals have been identified. Taking into account that these rocks are considered as commonly used local building material, being utilized also for the construction of the medieval and pre-modern historical monuments from the city of Iasi, the study draws attention to the detailed assessment of their conservation status from the built heritage in relation to the surrounding environment.*

*Keywords: porous geomaterials, lithic surface, atmospheric pollution, radionuclides, building heritage*

In the last decades, changes in the urban environment and its influences on the historical buildings are present in many forms such as: evolutionary, deterioration and/or degradation effects of the lithic materials used in their construction [1 - 3]. A feature strongly affected by atmospheric pollution is the colour of the apparent surfaces, a phenomenon intensively studied globally [4, 5], followed by the degree of fragility by changing the composition in chemically-bound water (leachable water).

This paper continues the study of the evolution of the chemical composition of some porous indigenous carbonate rocks exposed in the urban environment, which among others factors it is influenced directly by the intense car traffic [6], but also by the presence of heavy metals in the street dust (road dust) [7] and residual traces of radionuclides present in the rock with undesirable effects on the historical monument located in the study area. The

study area, the Stone Bridge (Podul de Piatra) crossroad (47.158040 N, 27.575385 E) is a very important and frequently circulated on both the regional and national level, as it coincides with European Route E583. The intense traffic is caused by the proximity of some point of interests such as the railway station, regional bus station, one hypermarket, and three gas stations (figs. 1 and 2).

## Experimental part

### Materials and methods

The geomaterials used in this study are porous oolitic carbonate rocks (fig. 3), generically named in the literature, since 1862: *Calcare de Repedea* [8]. Recent studies [9] have shown that they are actually fossilized sandstones. The analysed samples come from the Paun - Repedea quarry, Iasi County, marked from P1 to P6 (six samples from the same rock - fig. 4), which were exposed for 124 days in the urban environment between October 2016 and



Fig. 1. Podul de Piatra (Stone Bridge) intersection from Iasi, Romania: a - older (historical) bridge; b - newer bridge; c - geographical position for exposure area [6]



Fig. 2. Exposure place, near Podul de Piatra road junction, Iasi, Romania [6]

\*email: iulianab2001@gmail.com; ion.sandu@uaic.ro

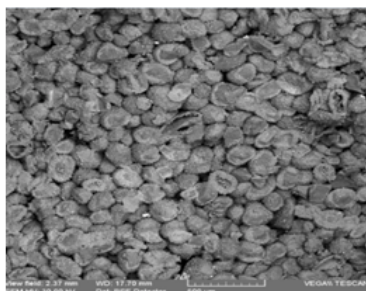


Fig. 3. SEM image (100x) on oolithical calcareous sample with porous surface [6]

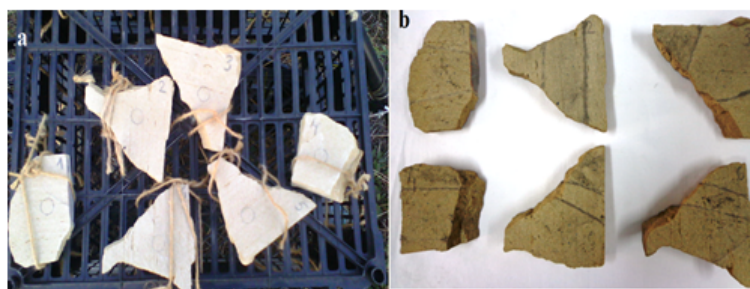


Fig. 4. Lithical porous samples: a - fresh calcareous rocks, before exposure period; b - after 124 exposure days (right image is obtained in laboratory conditions) [6]

Fig. 5. Porous oolithical carbonate rocks with long exposure time in urban environment in Stone Bridge junction (PPN- outer surface crust, altered; PPA- inner surface crust, unaltered)



Fig. 6. Blank sample - porous oolithical carbonate rocks (P0)

February 2017, for monitoring both the colour changes over time and the chemical composition changes in the exposed superficial structures relative to the unmodified chemical structure within the samples [6].

The six samples (P1-P6) included in the analysis were compared with a sample that has the old patina (PPN - outer surface and PPA - inner surface - breakage, fig. 5), that was taken from the historical monument located in the experimental area and with a blank sample (P0, fig. 6) taken simultaneously with the first six from the Paun - Repedea quarry. All samples are carbonate rocks with a similar petrographic structure. The samples were subjected to CIE  $L^*a^*b^*$  colorimetry, SEM-EDX, LA-ICP-MS and LIBS instrumental analyses both on the outside and inner part, except for the blank sample that has not been exposed to environmental factors, being kept under constant laboratory conditions in a dark-coloured desiccator.

#### CIE $L^*a^*b^*$ colorimetry

CIE  $L^*a^*b^*$  colorimetry was done using a Lovibond® RT 300 spectrophotometer (Reflectance Tintometer D65/10°) which allowed the measuring of the chromatic modifications, in the exact same spots, for the entire duration of the investigation. CIE  $L^*a^*b^*$  colorimetry method was applied for samples P5 and P6 due to its extreme colour variation.

#### SEM - EDX analysis

The analysis of samples (composition and micro-structural morphology) was carried out using a scanning electron microscope (SEM), model VEGA II LSH, produced by TESCAN® Czech Republic, coupled with an EDX QUANTAX QX2 detector, manufactured by BRUKER/ROENTEC® Germany. Sample analysis was performed at 100 to 2500X magnification with an accelerating voltage of 30 kV, and the working pressure was less than  $1 \times 10^{-2}$  Pa.

Table 1  
TYPICAL OPERATION PARAMETERS OF LA-ICP-MS ANALYSIS

ICP-MS		Laser Ablation System	
Model	Agilent 7700X	Model	LSX-266 (CETAC)
RF power	1550 W	Wavelength	266 nm
Carrier gas	1.01 L·min <sup>-1</sup> (Ar)	Laser frequency	20 Hz
Auxiliary gas	0.7 L·min <sup>-1</sup> (Ar)	Spot diameter	25 μm
Carrier gas	1.27 L·min <sup>-1</sup> (Ar)	Ablation pattern	line
Plasma gas	15 L·min <sup>-1</sup> (Ar)	Background time	20 s
Cones	Ni (sampler and skimmer)	Ablation time	80 s
Detector mode	Dual-pulse counting and analog		
Isotope Measured	7Li; 45Sc; 51V; 52Cr; 55 Mn; 59Co; 63Cu; 66Zn; 69Ga; 85Rb; 88Sr; 89Y; 90Zr; 95Mo; 133Cs; 138Ba; 139La; 140 Ce; 141Pr; 146Nd; 147Sm; 153Eu; 157Gd; 159Tb; 165Ho; 169Tm; 172Yb; 175Lu; 178Hf; 208Pb; 232Th; 238U		
Reference material	BCR2G (USGS)		

The resulting image was formed by secondary electrons (SE) and backscatter electrons (BSE).

#### LA-ICP-MS system for isotope analysis

For the ablation of solid porous geomaterials was used a LA-ICP-MS system, which focused a laser beam in an inert gas environment such as Ar, at normal pressure followed by the transfer of ablated material in a continuous flow of He and Ar to the ICP-MS [10]. For the present study, the analysis of trace elements and REE were carried out using a solid state Nd-YAG laser ablation systems CETAC LSX-266 coupled with Agilent 7700x ICP-MS [11]. The LA-ICP-MS optimization was obtained with NIST612 glass reference material. Since marble standards are not available, calibration is performed using BCR 2G glass reference materials as external standards. All procedures for data acquisition were those normally used in the Mass Spectroscopy Laboratory of the CERNESIM Department, Alexandru Ioan Cuza University of Iasi - Romania [12]. The operation parameters for the LA-ICP-MS system are presented in table 1.

For all analyses, a transient signal of intensity versus time was obtained for each element using 20-s background levels (acquisition of gas blanks) followed by 80 s of ablation and then 60 s of post-ablation at background levels [13-14]. The relative element sensitivity for each element was calculated using modified Longerich equation for three replicates.

The environmental impact of metals and the pollution level in the porous geomaterials can be determined with the help of two parameters; the *Enrichment Ratio* (ER) and the *Geoaccumulation Index* ( $I_{geo}$ ).

*Enrichment Factor* (EF), is a tool for assessing the enrichment degree and comparing the contamination of different environmental media. It normalizes metal concentration as a ratio to another element from the studied samples, in according with formula [15, 16]:

$$EF = (C_M/C_{Mo})_{sample} / (C_M/C_{Mo})_{background}$$

where:

$(C_M/C_{Mo})_{sample}$  is the ratio of metal and molybdenum (Mo) concentrations in the sample,

$(C_M/C_{Mo})_{background}$  is the ratio of metal and molybdenum (Mo) concentrations of the background.

The element selected should be associated with finer particles and its concentration should not be highly influenced by the anthropogenically input. For the present study, it has been selected to normalise metal concentrations the molybdenum (Mo) for trace elements and lutetium (Lu) for rare earth.

The world average from upper continental crust and the world average from limestone are among the materials often used to provide background metal levels. Literature

indicates for EF values that range between 0.5 and 1.5 that the metal source is entirely from crustal materials or natural processes, whereas EF values greater than 1.5 suggest anthropogenic sources [17].

*Geoaccumulation Index* ( $I_{geo}$ ) - assesses the pollution level of the studied elements and is computed [18]:

$$I_{geo} = \log_2 \left[ \frac{C_n}{1.5 \times B_n} \right]$$

where:

-  $C_n$  is the measured concentration of the element in environment,

-  $B_n$  is the geochemical background value in soil and

- 1.5 is the correction factor of background due to lithological effects.

#### Laser-Induced Breakdown Spectroscopy - LIBS

A part of the analysis was performed using a Laser-Induced Breakdown Spectroscopy Technique (LIBS) with an Acton 2750i high resolution spectrometer (750 mm focal length) coupled with an Intensified Roper Scientific PIMAX3 ICCD camera 1024 × 1024 pixels with a minimum gate time of 2 ns. The experimental device is designed to study laser-induced ablation plasma, time and space-resolved optical emission spectroscopy with applications for environmental and Pulsed Laser Deposition Techniques (PLD) [19 - 21]. Plasma laser ablation was performed by irradiating the various samples placed in a vacuum chamber providing a working gas pressure of up to 10<sup>-8</sup> Torr. Plasma obtained by laser ablation has a translation motion along a direction perpendicular to the surface of the irradiated samples, the expansion direction being parallel to the slit of the Acton spectrometer. In this case, the integrated LIBS specimens can be recorded after the full extent of the plume so that the technique ensures a very high trace detection limit. Optical radiation used for ablation was obtained from a laser Nd: Yag laser (Quantel Brilliant Eazy, 532 nm, 10Hz repetition rate, pulse width 10 ns). The radiation beam was focused on the sample with a convergent lens with a focal length of 10 cm placed in the vacuum chamber. The sample was continuously moved by a computerized system providing a 3D micrometric shift. The energy/pulse employed were 100 mJ, for an impact spot diameter of 0.4 mm leading to a fluence of 800 J/cm<sup>2</sup>. Several spectral domains have been recorded that have shown increased attention depending on the chemical species present in the sample and their intensity (concentration, spectroscopic characteristics, etc.)

#### Results and discussions

After 124 days of exposure of the P1-P6 samples (taken from the quarry - fig.4) to the environmental factors in the area surrounding the monument, these as well as the

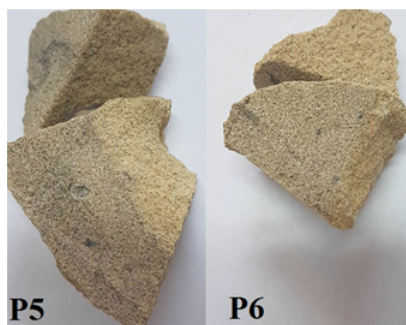


Fig. 7. Porous oolithic carbon rock samples: P5 ( $\Delta E^*_{ab} = 11.39$ ) and P6 ( $\Delta E^*_{ab} = 7.26$ ) [6]

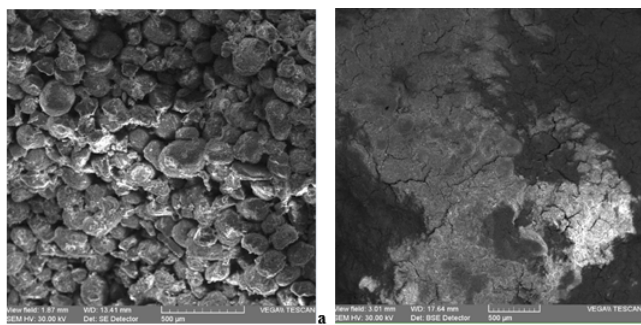


Fig. 8. SEM image (100X bse) on oolithic calcareous samples with porous surface: a - inner lithic surface, unaltered - PPA; b - external crust, exposed to urban environment conditions - PPN

Elements	Sample P5 ( $\Delta E^*_{ab} = 11.39$ )				Sample P6 ( $\Delta E^*_{ab} = 7.26$ )			
	% atomic		% weight		% atomic		% weight	
	inside	outside	inside	outside	inside	outside	inside	outside
Calcium	32.08	21.48	48.96	35.55	29.79	32.09	46.20	46.82
Silicon	12.90	14.14	13.80	16.41	12.33	19.47	13.39	19.91
Aluminum	0.97	1.65	0.99	1.84	1.23	1.76	1.29	1.72
Carbon	0.24	0.75	0.11	0.37	0.26	0.13	0.12	0.06
Iron	0.70	0.76	1.49	1.75	0.65	0.79	1.42	1.59
Manganese	0.37	0.31	0.77	0.70	0.30	0.00	0.61	0.00
Potassium	1.57	1.13	2.34	1.83	1.50	2.47	2.27	3.52
Magnesium	0.65	1.02	0.60	1.02	0.93	0.74	0.87	0.66
Sodium	0.60	1.84	0.52	1.74	0.87	0.94	0.77	0.79
Oxygen	49.93	55.52	30.42	36.68	51.31	40.85	31.76	23.79
Sulfur	0.00	0.59	0.00	0.79	0.00	0.33	0.00	0.39
Chlorine	0.00	0.53	0.00	0.77	0.00	0.00	0.00	0.00
Titanium	0.00	0.28	0.00	0.55	0.46	0.43	0.85	0.75
Phosphorus	0.00	0.00	0.00	0.00	0.37	0.00	0.45	0.00
Total	100	100	100	100	100	100	100	100

**Table 2**  
SEM-EDX - ELEMENTAL COMPOSITION IN PERCENTAGE (INSIDE VS. OUTSIDE) FOR LITHICAL SAMPLES P5 AND P6, AFTER 124 EXPOSURE DAYS [6]

Elements	Sample PPA (inside)		Sample PPN (outside, black crust)	
	% atomic	% weight	% atomic	% weight
Calcium	31.03	48.71	5.11	9.83
Silicon	9.18	10.10	15.38	20.74
Aluminum	1.57	1.66	4.66	6.02
Carbon	0.20	0.09	3.03	1.75
Iron	0.54	1.19	1.29	3.44
Manganese	0.00	0.00	0.00	0.00
Potassium	2.08	3.19	1.89	3.57
Magnesium	1.06	1.00	1.10	1.29
Sodium	0.00	0.00	1.02	1.13
Oxygen	54.34	34.06	65.44	50.26
Sulfur	0.00	0.00	0.29	0.44
Chlorine	0.00	0.00	0.00	0.00
Titanium	0.00	0.00	0.42	0.98
Phosphorus	0.00	0.00	0.37	0.55
Total	100	100	100	100

**Table 3**  
SEM-EDX - ELEMENTAL COMPOSITION IN PERCENTAGE FOR LITHICAL SAMPLES PPA AND PPN

naturally aged PPN/PPA sample (fig. 5) and the reference sample P0 (fig. 6) were analyzed by CIE  $L^*a^*b^*$  colorimetry, SEM-EDX, LA-ICP-MS and LIBS. Of these samples, following the CIE  $L^*a^*b^*$  colorimetry study, only two were selected [6], with the minimum value of the color change in the CIE  $L^*a^*b^*$  system from sample P6 ( $\Delta E^*_{ab} = 7.26$ ) and respectively the sample P5 with the maximum value ( $\Delta E^*_{ab} = 11.39$ ) shown in figure 7.

#### SEM - EDX results

For the comparative study of SEM-EDX elemental chemical composition, only samples P5 and P6 (fig. 7), respectively PPN (black patina) and PPA (in the region with the interior structure, unaffected by the environmental factors - fig. 5). Using Scanning Electron Microscopy (SEM) coupled with Energy Dispersive X-ray Spectroscopy (EDX), provided information on the morphology and elemental composition of Porous Calcareous Rocks and External Crust. SEM images of the external and internal surfaces of the samples and the chemical elemental compositions determined from the EDX spectra are presented in figure 8 and tables 2 and 3.

According to the elemental analysis data from tables 2 and 3 for the two areas, the one affected by the environmental factors and the internal structures of the analyzed SEM-EDX samples, the following observations can be made:

- the P5 sample, most affected by environmental factors in terms of color change, has large compositional differences with inside vs. outside structures for: calcium, magnesium and potassium. If there is an analysis for the exterior vs. interior structures, the biggest differences are: silicon, aluminium, carbon, sulphur, chlorine and titanium, caused by a rate of contamination with street dust, saline aerosols and poisoning (combustion gases);

- the P6 sample least affected by environmental factors in terms of colour change shows large differences in composition for inside structures than outside ones such as carbon, manganese, magnesium, titanium, and phosphorus. For outside vs. inside surface, there are differences for: calcium, silicon, aluminium, iron, potassium, sodium, sulphur, determined by a lower rate of contamination at first sight because of the increased presence of calcium and sulphur will increase the degree

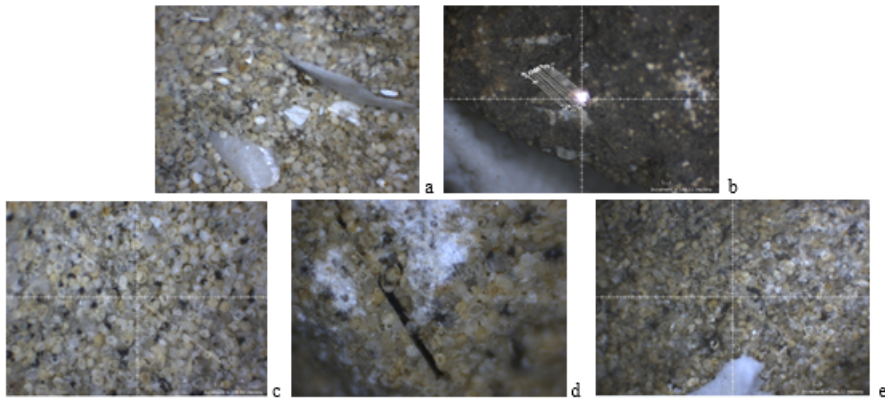


Fig. 9. The LA- ICP-MS areas of analysis: a – PPA; b – PPN; c – P0; d – P5; e – P6

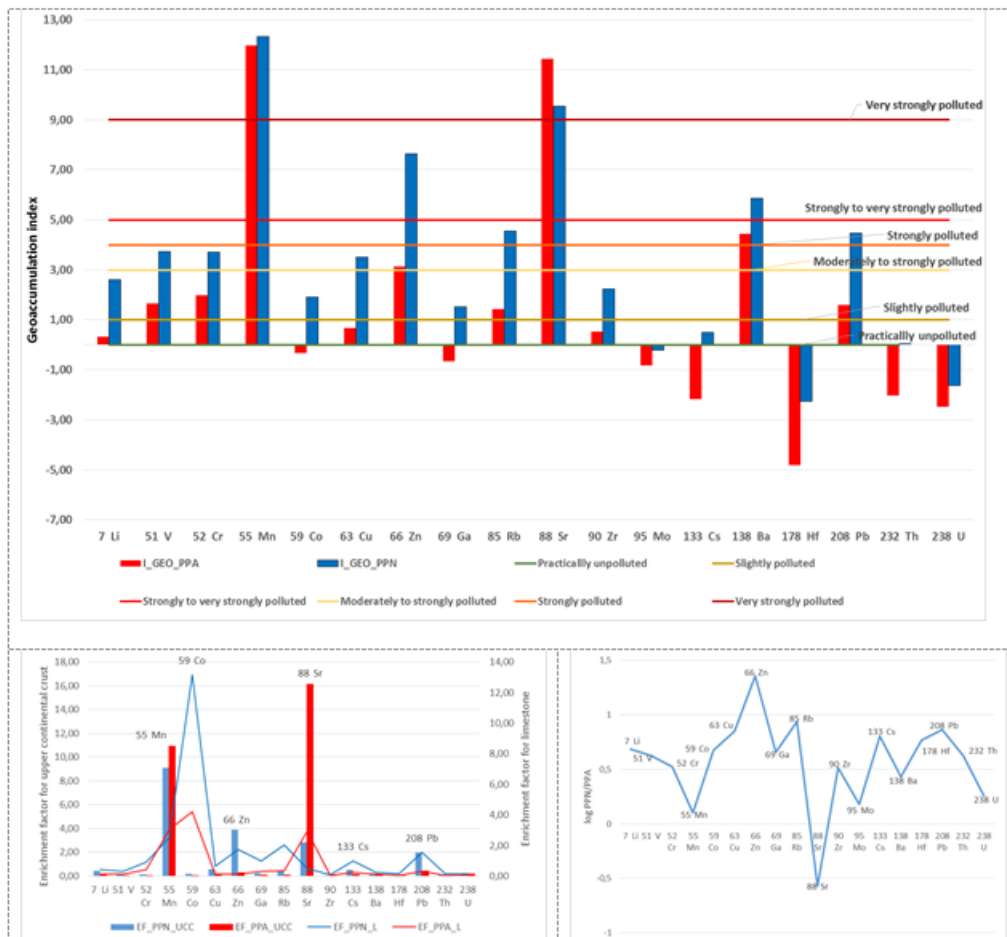


Fig.10. Geoaccumulation index ( $I_{geo}$ ), enrichment factor and normalized curve of heavy metals, lithophile and radionuclides elements in porous geomaterials (for PPA and PPN samples)

of white by the presence of sulphates, and the manganese from the interior decreases the degree of white;

-the PPA vs PPN sample exhibits increased compositional differences in inside vs. outside structures only for calcium and potassium;

-the PPN vs. PPA sample exhibits increased compositional differences with external structures than internal ones for a wide range of elements: silicon, aluminium, carbon, iron, sodium, sulphur, titanium and phosphorus, which are responsible for the formation of the aging patina.

#### LA-ICP-MS results

LA- ICP-MS data provides useful information concerning the type and source of altered crusts from the surface. The calculated geoaccumulation index puts into evidence higher values of both trace and rare elements, which are lower in the initial sample, mostly due to the exposure in the urban environment (traffic, increase radioactivity levels). For the determination of chemical compositions by LA-ICP-MS on samples P0, P5, P6, PPN and PPA, figure 9 shows the areas

of analysis, while figures 10 and 11 show geoaccumulation index diagrams ( $I_{geo}$ ) in correlation with the enrichment factor (EF). Some trace and minor elements (such as V, Cr, Mn, Co, Cu, Zn, Ga, Rb, Sr, Zr, Mo, Cs, and Ba) occurring in very small concentrations or totally lacking in the substrate are very significant for understanding the genesis of altered crusts. The mean values of element concentrations in altered outer surface of crusts (PPN) were normalized with the corresponding mean value of the inner surface crust unaltered porous geomaterials (PPA). Generally, except for Mn, Sr, Mo, and U which have concentrations comparable with those in the unaltered porous geomaterials (altered crusts /unaltered porous geomaterials ratio close to 1), substantial differences in the enrichment factor can be observed. For a better assessment of the enrichment or depletion degree of the elements in altered crusts with respect to unaltered samples, logarithmic plots for all elements are presented.

#### LIBS results

The elemental compositions were analyzed on the part unaffected by pollution (P0) and outside areas (P5 and

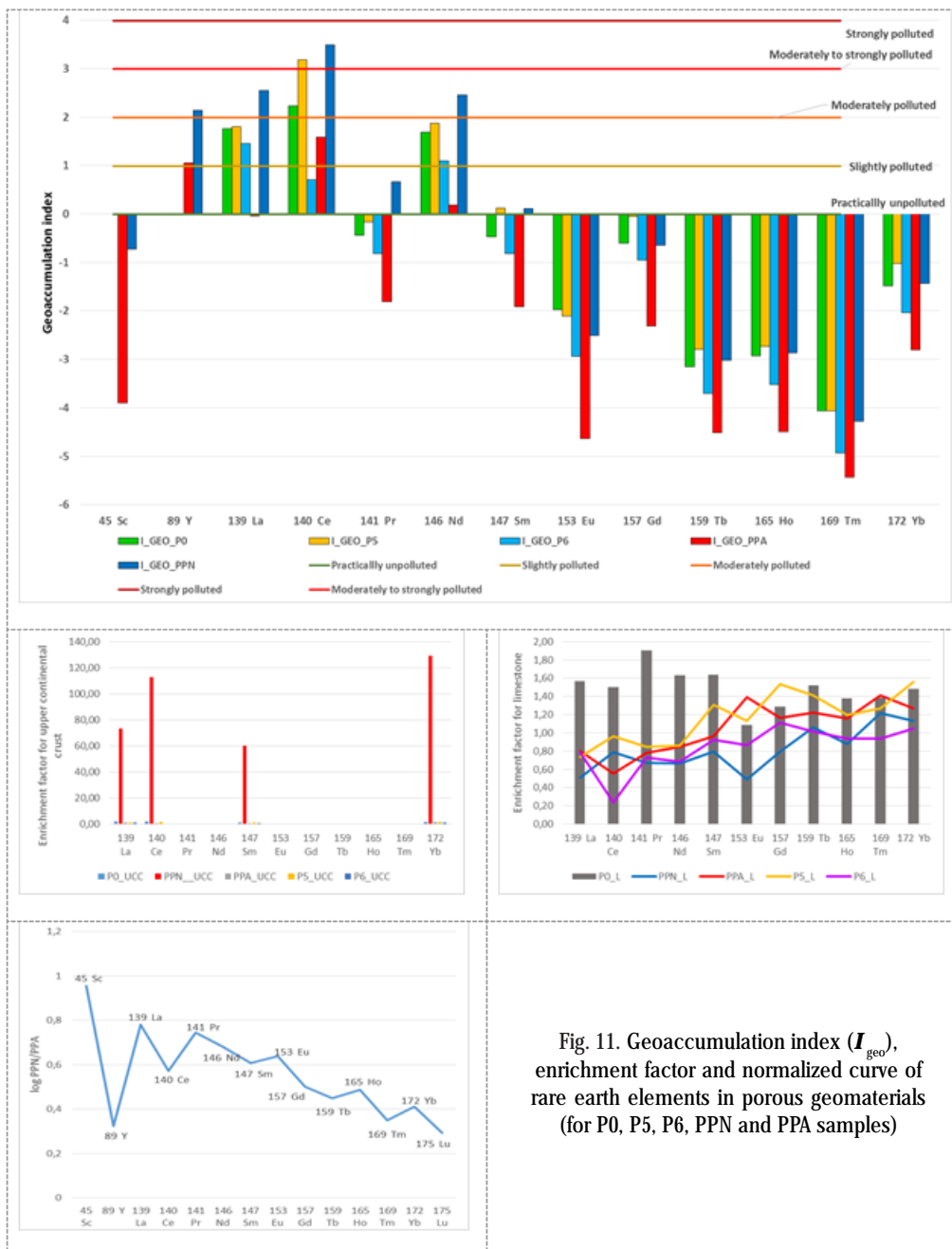


Fig. 11. Geoaccumulation index ( $I_{geo}$ ), enrichment factor and normalized curve of rare earth elements in porous geomaterials (for P0, P5, P6, PPN and PPA samples)

P6), keeping the same experimental conditions. In figure 12 there is an overview of the 365-675 nm spectral range.

This technique allows to highlight the common chemical elements of the remaining traces of radionuclides, so the three samples P0, P5 and P6 contain a series of common elements such as: carbon, silicon, iron, titanium, zirconium, chromium, tin, calcium and sodium. Most of these are

derived from the base rock, but also from chemical pollution, respectively those of radioactive contamination: iodine, cesium, osmium, thorium, terbium, berkelium, holmium, samarium, and indium.

Radionuclides from the aerosols, regions dust, cosmic dust, nuclear accidents or mining area [22 – 27] are taken over by meteoric water [28] and at the lithosphere level [29] are retained in time by the alumino-silicate, titanate, ferrates, etc. structures present in the sedimentary rocks.

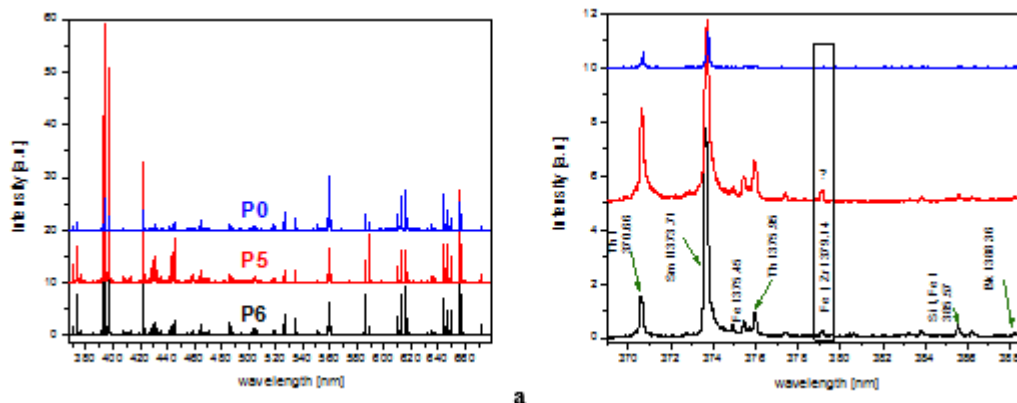


Fig. 12. Optical emission spectra of laser ablation plasma for investigated samples. The integration time was 2 microseconds for each spectral range: a. 370-675 nm; b. 370-388 nm

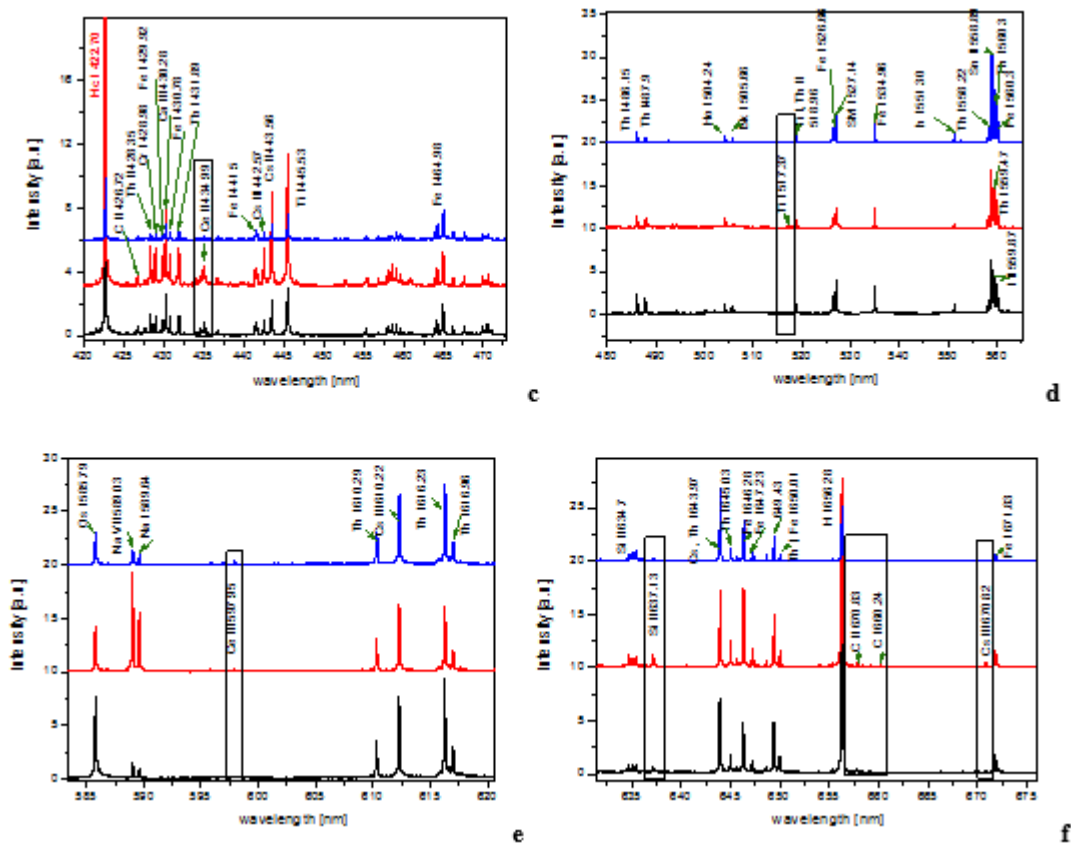


Fig. 12. Optical emission spectra of laser ablation plasma for investigated samples. The integration time was 2 microseconds for each spectral range: c. 420-475 nm; d. 480-565 nm; e. 585-620 nm; f. 630-675 nm

These structures contain acidic groups of the type Si(IV)-OH<sup>-</sup>, Ti(IV)-O<sup>-</sup>, Fe(≥III)-O-H<sup>+</sup>, etc., capable of ion exchange for heavy metal and radionuclide cations. The evolution over time of retained radionuclides is dependent on their radioactive activity, chemical load and pH of meteoric and groundwater. Some radionuclides have high stability, and others are sensitive to environmental fluctuations. Due to the disintegration, the radionuclides retained in the rock act on leachable waters (chemically bonded) generating HO· free radical formation processes, which in time yield oxidative processes by which Fe(II, III), Mn(II, III) ions, etc. They pass into higher oxidation states, leading to a pronounced change in color (to brownish black). Also, due to water loss due to the radiolysis processes, the alumina and silicate polyhedrons are structurally reformulated, generating significant chromatic deviations in superficial structures.

## Conclusions

Combining four instrumental techniques (CIE L\*a\*b\* colorimetry, SEM-EDX, LIBS, and LA-ICP-MS) in assessing the impact of environmental factors on the porous carbonate rocks from the traditional Paun Repedea quarry (Iasi County), used over the years as a building material for monuments in Iasi, the following conclusions can be drawn:

- CIE L\*a\*b\* colorimetry analysis highlights the impact of current environmental factors with high aggressiveness caused by very intense road traffic and the concentration of air and ascendant currents on the Bahlui riverbed in the area of a monument near which it was installed a platform with 6 samples of the same type of geomaterials by differentiating the chemical elements common from those of contamination;

- from the samples taken into the study by CIE L\*a\*b\* colorimetry, only two were selected, with the minimum value of the colour change in the CIE L\*a\*b\* system from sample P6 ( $\Delta E^*_{ab} = 7.26$ ) and respectively the sample P5 with the maximum value ( $\Delta E^*_{ab} = 11.39$ ), together

with a blank sample P0 and one with the patina from the monument, PNN / PNA, which were analysed with SEM-EDX, LA-ICP-MS and LIBS, to emphasize the role of common chemical elements, residual traces of radionuclides and current contamination on the effects of aging;

- an important role regarding the aging of the lithic materials used in construction of the monument is the aggressiveness of the current urban pollution and the reactivation of some remaining radionuclides, leading to segregation of some microelements, structural reforming of aluminosilicates, carbonates, sulphates and phosphates by water-leach loss and oxidation of polyvalent cations in higher states following the chemically bonded water radiolysis and crystallization or co-ordination processes, with colour change and monolithisation of deposits.

*Acknowledgments: We are grateful to Dr Viorica VASILACHE, Dr Mihai Marius CAZACU and Oana RUSU, from the Alexandru Ioan Cuza University of Iasi - Romania, for all the support given in the experiments and the suggestions given in the elaboration of this paper.*

## References

1. FOOKES, P.G., Quarterly Journal of Engineering Geology, **24**, no. 1, 1991, p. 3.
2. CAMUFFO, D., The Science of the Total Environment, **167**, 1995, p. 1.
3. TORRERO, E., SANZ, D., ARROYO, M.N., NAVARRO, V., International Journal of Conservation Science, **6**, no. 4, 2015, p. 625.
4. GROSSI, D., DEL LAMA, E.A., GARCIA-TALEGON, J., INIGO, A.C., VICENTE-TAVERA, S., International Journal of Conservation Science, **6**, no. 3, 2015, p. 313.
5. PELIN, V., SANDU, I., GURLUI, S., BRANZILA, M., VASILACHE, V., SANDU, I.G., Rev. Chim. (Bucharest), **51**, no. 12, 2016, p. 2568.
6. PELIN, V., RUSU, O., SANDU, I., VASILACHE, V., GURLUI, S., SANDU A.V., CAZACU M.M SANDU, I.G., IOP Conf. Series: Materials Science and Engineering, **209**, 2017, Article No. 012080, doi:10.1088/1757-899X/209/1/012080.

7. BREABAN, I.G., PAIU, M., International Multidisciplinary Scientific Geoconference – SGEM, **2**, 2016, p.79.
8. COBALCESCU, G., Revista Romana Pentru Stiinte, Litere si Arte, **2**, 1862, p. 585.
9. GRASU, C., BRANZILA, M., MICLAUS, G.C., BOBOS, I., Sarmatianul din sistemul bazinelor de foreland ale Carpatilor Orientali, Ed. Tehnica, Bucuresti, 2002.
10. PICKHARDT, C., DIETZE, H.J., BECKER, J.S., International Journal of Mass Spectrometry, **242**, 2005, p.273.
11. BRATZ, H., KLEMD, R., Agilent Technologies, 2002, Article ID **5988-6305EN**, <http://www.agilent.com>.
12. BREABAN, I.G., PAIU, M., JURAVLE, D.T., International Multidisciplinary Scientific Geoconference - SGEM, **1**, 2016, p.297.
13. BARCA, D., BELFIORE, C.M., CRISCI, G.M., LA RUSSA, M.F., PEZZINO, A., RUFFOLO, S.A., Environmental Science And Pollution Research, **17**, no. 8, 2010, p. 1433.
14. GUNTHER, D., HATTENDORF, B., TrAC Trends in Analytical Chemistry, **24**, no. 3, 2005, p. 255.
15. YONGMING, H., PEIXUAN, D., JUNJI, C., POSMENTIER, E.S., Sci. Total Environ., **355**, 2006, p. 176.
16. LU, X., WANG, L., LEI, K., HUANG, J., ZHAI, Y., Journal of Hazardous Materials, **161**, No. 2-3, 2009, p. 1058.
17. MULLER, G., Geol. J., **2**, 1969, p. 108.
18. ZHANG, W.G., FENG, H., CHANG, J.N., QU, J.G., XIE, H.X., YU, L.Z., Environmental Pollution, **157**, no.5, 2009, p. 1533.
19. COCEAN, A., PELIN, V., CAZACU, M.M., COCEAN, I., SANDU, I., GURLUI, S., IACOMI, F., Applied Surface Science, 2017, in print, <https://doi.org/10.1016/j.apsusc.2017.03.172>
20. GRADINARU, I., TIMOFTE, D., VASINCU, D., TELSOIANU, D., CIMPOESU, R., MANOLE, V., GHEUCA-SOLOVASTRU, L., Mat. Plast., **51**, no.3, 2014, p. 230.
21. TEODORESCU, M., SCHACHER, L., ADOLPHE, D., GRADINARU, I., ZETU, I., STRATULAT, S., Mat. Plast., **50**, no.3, 2013, p. 225.
22. STRODE, S.A., OTT, L.E., PAWSON, S., BOWYER, T.W., Journal of Geophysical Research, **117**, 2012, Article No. D09302.
23. HAYES, C.T., ROSEN, J., MCGEE, D., BOYLE, E.A., Global Biogeochemical Cycles, **31**, no.2, 2017, p. 238.
24. TOMASEK, M., RYBACEK, K., WILHELMOVA, L., Journal of Radioanalytical and Nuclear Chemistry-Letters, **201**, no. 5, 1995, p. 409.
25. ONDOV, J.M., KELLY, W.R., Analytical Chemistry, **63**, no. 13, 1991, p. A691.
26. WANG, L.Q., ZHONG, B.Q., LIANG, T., XING, B.S., ZHU, Y.F., Science of the Total Environment, **572**, 2016, p. 1.
27. <http://www.world-nuclear.org/information-library.aspx>
28. SAKUMA, K., KITAMURA, A., MALINS, A., KURIKAMI, H., MACHIDA, M., MORI, K., TADA, K., KOBAYASHI, T., TAWARA, Y., TOSAKA, H., Journal of Environmental Radioactivity, **169**, 2017, p. 137.
29. BIHARI, A., DEZSO, Z., Journal of Environmental Radioactivity, **99**, no. 7, 2008, p.108.

---

Manuscript received: 28.12.2016